ARTICLES

Ab Initio Molecular Orbital Calculations on $NO^+(H_2O)_n$ Cluster Ions. 2. Thermodynamic Values for Stepwise Hydration and Nitrous Acid Formation†

Essam Hammam,‡,§ E. P. F. Lee,‡,|| and J. M. Dyke*,‡

Department of Chemistry, The University of Southampton, Highfield, Southampton SO17 1BJ, U.K., Chemistry Department, Tanta University, Tanta, Egypt, and Department of Applied Biology and Chemical Technology, Hong Kong Polytechnic University, Hung Hom, Hong Kong

Received: October 19, 2000

Ab initio molecular orbital calculations have been used to compute thermodynamic constants ($\Delta H°$, $\Delta S°$, $\Delta G°$) for the stepwise hydration reactions of $NO^+(H_2O)_n$ and for the competing rearrangement reaction which produces HONO and $H^+(H_2O)_n$ (for $n \leq 4$). Geometry optimizations and harmonic frequency calculations were performed at the MP2/6-311++G(2d,p) level, and relative energies were computed at the MP2/aug-cc-pVTZ level with MP2/6-311++G(2d,p) optimized geometries. The geometry changes and energetics of these competing solvation and rearrangement reactions have been studied, and reasons are proposed to explain why $NO^+(H_2O)_{n+1}$ formation is the dominant process for $n = 1$ and $n = 2$ but HONO + $H^+(H_2O)_n$ formation contributes for $n = 3$ and becomes more important for $n = 4$.

1. Introduction

Of the species present in the earth's atmosphere,[1] the comparatively low first ionization energy of NO means that NO^+, formed by photoionization by solar radiation or charge transfer, is the major primary ion. One of the issues of current interest in the chemistry of the upper atmosphere concerns formation of other ions from NO^+ below ≈90 km−in particular the routes of production of proton hydrates $H^+(H_2O)_n$ from NO^+. It has been proposed[2,3] that NO^+ participates in a series of two- and three-body ion−molecule switching reactions with water and other small molecules, such as N_2 and CO_2, with the final two steps in the sequence being

$$NO^+(H_2O)_n + H_2O \rightarrow NO^+(H_2O)_{n+1} \quad (1)$$

$$NO^+(H_2O)_n + H_2O \rightarrow HONO + H^+(H_2O)_n \quad (2)$$

There is experimental evidence[4−6] to suggest that reaction 1 is the dominant reaction for $n = 1$ and 2 and reaction 2 starts to play a role for $n = 3$ and becomes dominant for $n = 4$.

In an earlier paper from this laboratory,[7] minimum energy geometries, harmonic vibrational frequencies, and stepwise binding energies have been computed for the cluster ions $NO^+(H_2O)_n$, for $n = 1-4$. Also, mechanisms for nitrous acid (HONO) formation when water is added to $NO^+(H_2O)_3$ and $NO^+(H_2O)_4$ have been established. The aim of this first paper was to establish a reliable and economical level of *ab initio* calculations for use on $NO^+(H_2O)_n$ complexes and to identify the mechanisms of HONO and $H^+(H_2O)_n$ formation when H_2O is added to $NO^+(H_2O)_3$ and $NO^+(H_2O)_4$.

In this first paper,[7] systematic *ab initio* calculations on the lighter $NO^+(H_2O)_n$ complexes ($n = 1$ and 2) at MPn, CCSD and CCSD(T) levels of electron correlation with different basis sets showed that the MP2/6-311++G(2d,p) level of theory was reliable for the calculation of minimum-energy geometries and harmonic vibrational frequencies. This level of theory was then used for the heavier complexes $NO^+(H_2O)_3$ and $NO^+(H_2O)_4$. Relative electronic energies were evaluated at the MP2/aug-cc-pVTZ//MP2/6-311++G(2d,p) level. The inclusion of zero point energy (ZPE) corrections, as well as counterpoise corrections for basis set superposition error (BSSE), in the calculation of binding energies was found to be essential to obtain the correct energy ordering for the different isomers of an $NO^+(H_2O)_n$ ionic complex.

This second paper reports the results of the computed thermodynamic constants ($\Delta H°$, $\Delta S°$, and $\Delta G°$) for the stepwise hydration of $NO^+(H_2O)_n$ ($n = 1-4$) (reaction 1) and for the intracluster reaction which produces HONO and $H^+(H_2O)_n$ (reaction 2) using the methods and basis sets of the earlier paper.[7] The aim is to understand the competition between reactions 1 and 2, in particular why reaction 2 becomes competitive with reaction 1 at $n = 3$ and dominant at $n = 4$.

2. Computational Details

The methodology employed in this work followed that of part 1.[7] In summary, geometry optimization and harmonic vibrational frequency calculations were performed at the MP2/6-311++G(2d,p) level, and relative energies were computed at the MP2/aug-cc-pVTZ level with the MP2/6-311++G(2d,p) geometries. In addition, more reliable energy calculations were carried out at the MP2/aug-cc-pVQZ//MP2/6-311++G(2d,p)

† Part of the special issue "Edward W. Schlag Festschrift".
* To whom correspondence should be addressed.
‡ Southampton University.
§ Tanta University.
|| Hong Kong Polytechnic University.

10.1021/jp003847q CCC: $20.00
Published on Web 01/26/2001

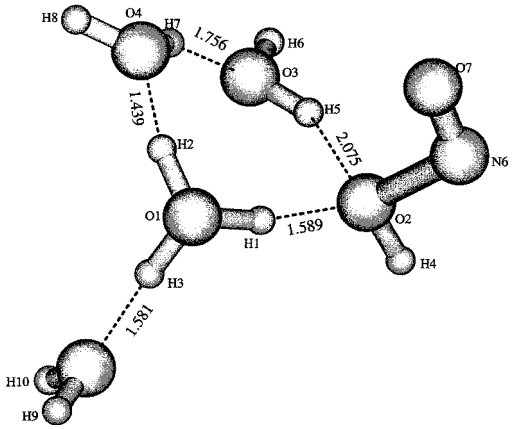

Figure 1. Reaction intermediate for the reaction $HONO{\cdot}H^+(H_2O)_3 + H_2O$.

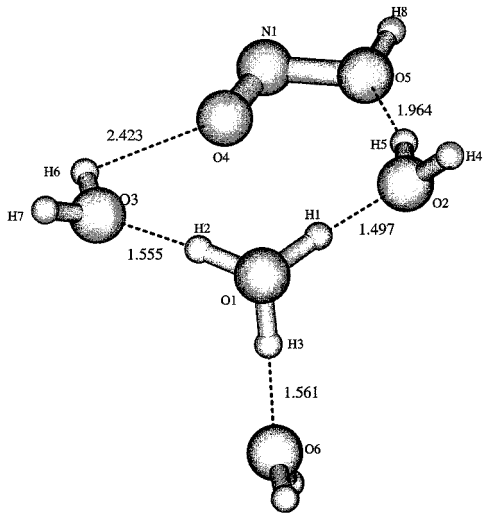

Figure 2. Product intermediate for the reaction $HONO{\cdot}H^+(H_2O)_3 + H_2O$.

level but only for the formation of the smaller complexes, $NO^+(H_2O)_{n+1}$, where $n + 1 = 1$ and 2.

Other than the $NO^+(H_2O)_{n+1}$ complexes, where $n + 1 = 1-4$, which were studied in part 1,[7] two isomeric structures of $HONO{\cdot}H^+(H_2O)_4$ (see Figures 1 and 2 and later text) were investigated in this work. Geometry optimization calculations were carried out at the MP2/6-311++G(2d,p) level. However, harmonic vibrational frequency calculations could not be carried out at this level, because the computational requirements were beyond the resources available to us. To characterize the nature of the minimum-energy structures obtained, MP2/6-31++G** geometry optimization and frequency calculations were carried out, employing the MP2/6-311++G(2d,p) geometry as the initial geometry. The optimized structures obtained at the MP2/6-31++G** and MP2/6-311++G(2d,p) levels are essentially identical. The MP2/6-31++G** frequency calculations on both structures gave all real vibrational frequencies, confirming that the structures obtained are true minima on the energy surface.

For reactions 1 and 2 with $n \leq 4$, reaction enthalpies ($\Delta H°$), entropies ($\Delta S°$), Gibb's free energies ($\Delta G°$), and equilibrium constants (K_p) were evaluated within the rigid-rotor harmonic-oscillator (RRHO) model. For reaction 1, interaction energies of complex formation were corrected for basis set superposition error (BSSE) using the full counterpoise method.[8] All the calculations were carried out using the GAUSSIAN 94 suite of programs.[9]

TABLE 1: Calculated Standard Thermodynamic Parameters[a] at 298 K for the Reaction $NO^+(H_2O)_n + H_2O \rightarrow NO^+(H_2O)_{n+1}$

$n+1$	$\Delta H°$(cp)/kcal mol^{-1}	$\Delta S°$/cal mol^{-1} K^{-1}	$\Delta G°$(cp)/ kcal mol^{-1}	K_p
		MP2/6-311++G(2d,p)		
1	−18.77	−23.42	−11.79	4.38×10^8
2	−14.75	−21.98	−8.19	1.01×10^6
3	−13.48	−40.81	−1.31	9.12
4	−11.22	−18.80	−5.61	1.29×10^4
		MP2/aug-cc-pVTZ//MP2/6-311++G(2d,p)		
1	−19.11	−23.42	−12.13	7.78×10^8
2	−14.67	−21.98	−8.12	8.95×10^5
3	−14.47	−40.81	−2.30	48.51
4	−10.99	−18.80	−5.38	8.78×10^3
		MP2/aug-cc-pVQZ//MP2/6-311++G(2d,p)		
1	−19.40	−23.42	−12.42	1.27×10^9
2	−14.90	−21.98	−8.35	1.32×10^6
		Experimental Values		
1	-18.5 ± 1.5,[b] -19.3 ± 2.4[c]	-23.0 ± 3[b]		
2	-16.1 ± 1.0[b]	-25.5 ± 2.5[b]		
3	-13.5 ± 1.0[b,d]			

[a] The $\Delta S°$ values are all obtained at the MP2/6-311++G(2d,p) level. [b] See ref 10. [c] See ref 11. [d] Extrapolated (see ref 10).

3. Results and Discussion

The computed thermodynamic quantities for the reactions investigated are summarized in Tables 1−3. In the following discussion, results obtained from the MP2/aug-cc-pVTZ//MP2/6-311++G(2d,p) level of calculation are referred to, unless otherwise stated. Results obtained at other levels of calculation are also given in Tables 1 and 3, to show the trend in the computed quantities as the level of calculation is improved. In general, on the basis of comparisons of the computed thermodynamic quantities obtained at different levels of calculation, it can be concluded that the best-computed values should be within the normally accepted chemical accuracy (±1 kcal mol^{-1} for energy; see also part 1[7])

3.1. Reaction 1: $NO^+(H_2O)_n + H_2O \rightarrow NO^+(H_2O)_{n+1}$. For reaction 1, the computed thermodynamic constants given in Table 1 were obtained with the reactants, $NO^+(H_2O)_n$, and the products, $NO^+(H_2O)_{n+1}$, in their respective lowest-energy isomeric structures (for the details of these structures, see part 1[7]). Experimentally derived reaction enthalpies, $\Delta H°$, and entropies, $\Delta S°$, are available for the $NO^+(H_2O)_{n+1}$ complex formation for $n + 1 = 1$, 2, and 3.[10,11] These experimental values were published a few decades ago, and some of them were reported with uncertainties larger than the normally accepted chemical accuracy of 1 kcal mol^{-1} for enthalpy and 1 cal mol^{-1} K^{-1} for entropy; one of them was obtained by extrapolation ($\Delta H°$ for $n = 3$; see footnote of Table 3 in ref 10). Despite these apparent shortcomings of the available experimental values, comparison between the computed and experimental values shows reasonably good agreement. However, it should be noted that, since a number of low-energy isomers have been found to be close in energy (see ref 7), the available experimental values (derived from mass-spectrometric data) are almost certainly affected by contributions from low-lying isomers. The effect of isomeric contributions on the experimental thermodynamic quantities is expected to be larger for the formation of the heavier clusters, as there would be more isomers of similar energy when the cluster size increases. In addition, the approximation of the RRHO model for floppy molecules would also lead to some errors in the computed thermodynamic quantities. Unfortunately, with the size of the systems considered here, it is not possible to exhaust the search of all isomeric

TABLE 2: Calculated Standard Thermodynamic Parameters at 298 K for the Reaction $NO^+(H_2O)_n + H_2O \rightarrow HONO + H^+(H_2O)_n$ with $n = 1-4$ at the MP2/6-311++G(2d,p) Level of Theory

reacn[a]	$\Delta H°$(cp)/kcal mol^{-1}	$\Delta S°$/cal mol^{-1} K^{-1}	$\Delta G°$(cp)/kcal mol^{-1}
$NO^+(H_2O) + H_2O \rightarrow HONO + H^+(H_2O)$	32.67	−8.58	35.23
$NO^+(H_2O)_2 + H_2O \rightarrow HONO + H^+(H_2O)_2$	13.11	−15.73	17.8
$NO^+(H_2O)_3 + H_2O \rightarrow HONO + H^+(H_2O)_3$	6.97	1.61	6.49
$NO^+(H_2O)_4 + H_2O \rightarrow HONO + H^+(H_2O)_4$	1.22	−8.85	3.85

[a] Using the most stable isomers.

TABLE 3: Calculated Standard Thermodynamic Parameters at 298 K for the Stepwise Hydration Processes That Lead to Nitrous Acid Formation[a]

reacn	$\Delta H°$(cp)/kcal mol^{-1}	$\Delta S°$/cal mol^{-1} K^{-1}	$\Delta G°$(cp)/kcal mol^{-1}	K_p
MP2/6-311++G(2d,p)//MP2/6-311++G(2d,p)				
(a) $NO^+ + H_2O \rightarrow NO^+(H_2O)$	−18.77	−23.42	−11.79	4.38×10^8
(b) $NO^+\cdot(H_2O) + H_2O \rightarrow NO^+(H_2O)_2$	−13.42	−27.32	−5.27	7.29×10^3
(c) $NO^+(H_2O)_2 + H_2O \rightarrow NO^+(H_2O)_3$	−10.02	−35.64	0.60	3.63×10^{-1}
(d) $NO^+(H_2O)_3 + H_2O \rightarrow HONO\cdot H^+(H_2O)_3$	−13.06	−30.60	−3.94	7.73×10^2
(e) $HONO\cdot H^+(H_2O)_3 \rightarrow HONO + H^+(H_2O)_3$	16.03	27.16	7.93	1.54×10^{-6}
(f) $NO^+(H_2O)_3 + H_2O \rightarrow HONO + H^+(H_2O)_3$	2.97	−3.44	3.99	1.19×10^{-3}
(g) $HONO\cdot H^+(H_2O)_3 + H_2O \rightarrow HONO + H^+(H_2O)_4$	−2.27	−2.11	−1.64	15.93
MP2/aug-cc-pVTZ//MP2/6-311++G(2d,p)				
(a) $NO^+ + H_2O \rightarrow NO^+(H_2O)$	−19.11	−23.42	−12.13	7.78×10^8
(b) $NO^+(H_2O) + H_2O \rightarrow NO^+(H_2O)_2$	−14.30	−27.32	−6.15	3.22×10^4
(c) $NO^+(H_2O)_2 + H_2O \rightarrow NO^+(H_2O)_3$	−11.29	−35.64	−0.67	3.09
(d) $NO^+(H_2O)_3 + H_2O \rightarrow HONO\cdot H^+(H_2O)_3$	−13.29	−30.60	−4.17	1.14×10^3
(e) $HONO\cdot H^+(H_2O)_3 \rightarrow HONO + H^+(H_2O)_3$	15.32	27.16	7.22	5.10×10^{-6}
(f) $NO^+(H_2O)_3 + H_2O \rightarrow HONO + H^+(H_2O)_3$	2.03	−3.44	3.05	5.81×10^{-3}
(g) $HONO\cdot H^+(H_2O)_3 + H_2O \rightarrow HONO + H^+(H_2O)_4$	−2.41	−2.11	−1.78	20.18

[a] Except for $NO^+(H_2O)_{n+1}$ with $n + 1 = 1$, the appropriate higher energy isomeric structures for $NO^+(H_2O)_{n+1}$ which lead to HONO formation (with negative $\Delta G°$ values) have been considered in this table. These structures arise from increasing the solvent chain bonded to NO^+ (see Figure 3; these are structure C_1(b) in Figure 1 and structure C_1(b) in Figure 2 of ref 7).

structures and/or go beyond the RRHO model. Nevertheless, it is pleasing to see that, for the cases shown in Table 1, discrepancies between the calculated and experimentally derived thermodynamic quantities are largely within experimental uncertainties.

Considering the stepwise hydration processes of NO^+ (reaction 1), it is clear from both the computed reaction enthalpies ($\Delta H°$) and free energies ($\Delta G°$), as shown in Table 1, that solvation of $NO^+(H_2O)_n$ (reaction 1) is thermodynamically favored, for $n = 1$ to 3 under standard state conditions (atmospheric pressure and room temperature). Considering the trends in the reaction enthalpies and free energies for stepwise solvation, the calculated values become less negative, as expected, when $n + 1$ increases from 1 to 3. However, for $n + 1 = 4$, the trend for $\Delta G°$ is reversed, as the $n + 1 = 4$ reaction 1 has a computed $\Delta G°$ value (−5.38 kcal/mol) which is more negative than that for $n + 1 = 3$ (−2.30 kcal/mol). This is despite the fact that the computed $\Delta H°$ value for $n + 1 = 3$ is −14.47 kcal/mol whereas that for $n + 1 = 4$ is −10.99 kcal/mol. The relatively small negative $\Delta G°$ value for $n + 1 = 3$ (−2.30 kcal.mol^{-1}) for reaction 1 arises mainly from the significant difference in the computed entropy values ($\Delta S°$) between $n + 1 = 3$ and 4. This can be understood in terms of the different geometrical structures of $NO^+(H_2O)_{n+1}$. As outlined in part 1,[7] the lowest-energy isomer with $n + 1 = 3$ has the third water molecule doubly hydrogen-bonded to two water molecules in the first solvation shell (thus starting the second solvation shell). However, with $n + 1 = 4$, the addition of the fourth water molecule is onto N of NO^+, filling up the first solvation shell. Thus, the unusual trend shown in the computed $\Delta G°$ values of the stepwise hydration processes of NO^+ may be understood in terms of structural considerations that the complexes being formed, with $n + 1 = 3$ and 4, have the addition of the last water molecules at very different sites. This has affected the standard entropy values for reaction that contribute to $\Delta G°$, with $\Delta S° = -40.81$ cal.mol^{-1}.K^{-1} for $n + 1 = 3$ and $\Delta S° = -18.80$ cal.mol^{-1}.K^{-1} for $n + 1 = 4$ (see Table 1). It has been pointed out in part 1[7] that the different hydrogen-bonding and water/NO^+ interactions are interrelated. The effects of these rather complex interrelated interactions, which are almost certainly nonadditive, seem to be reflected also in the magnitudes of the computed thermodynamic constants.

3.2. Reaction 2: $NO^+(H_2O)_n + H_2O \rightarrow HONO + H^+(H_2O)_n$. In Table 2, the computed thermodynamic constants for reaction 2 are listed, where all the species considered are in their lowest-energy isomeric structures. It is clear from the computed $\Delta H°$ and $\Delta G°$ values (all positive values) that all the reactions shown are thermodynamically unfavorable. This is so, even for $n = 4$. Although the more reliable MP2/aug-cc-pVTZ//MP2/6-311+G(2d,p) level of calculation has not been employed here, it is not expected that a higher level of calculation than the MP2/6-311+G(2d,p) level would change this conclusion, particularly for reactions with lower n values ($n \leq 4$). Nevertheless, it can also been seen that as the number of water molecules increases, the computed reaction enthalpies and free energies are becoming less positive. Again an interesting change in sign of $\Delta S°$ occurs between $n = 3$ and 4 (with $\Delta S°$ values for $n = 2$, 3, and 4 computed as −15.73, +1.61, and −8.85 cal mol^{-1} K^{-1}). These changes can as before be related to the structure of the $NO^+(H_2O)_n$ complexes. If the trend in $\Delta G°$ shown in Table 2 continued, it is expected that when n increases beyond 4, nitrous acid formation would become thermodynamically favored, for the lowest-energy isomers of $NO^+(H_2O)_n$. However, it will be shown in the following subsection that if some low-energy isomers of the lighter NO^+ hydrates are used, $HONO\cdot H^+(H_2O)_3$ can be formed via a barrierless reaction of $NO^+(H_2O)_3 + H_2O$; the subsequent reaction of $HONO\cdot H^+(H_2O)_3$ with H_2O, giving the separate products of HONO and $H^+(H_2O)_4$, is also thermodynamically favorable.

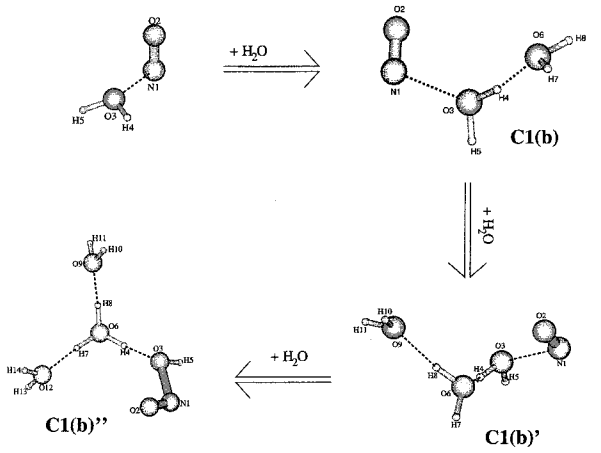

Figure 3. Hydration sequence of $NO^+(H_2O)$ which leads to the $HONO{\cdot}H^+(H_2O)_3$ adduct.

3.3. Formation of Nitrous Acid via the Stepwise Hydration Processes of NO^+. The computed thermodynamic values of the stepwise hydration reactions of NO^+ leading to the formation of HONO are listed in Table 3. In part 1,[7] it was shown that, with a suitable isomeric structure of $NO^+(H_2O)_3$, the addition of the fourth water at the appropriate site would lead to a barrierless reaction, which gives the $HONO{\cdot}H^+(H_2O)_3$ complex (Figure 3). The computed thermodynamic constants for the stepwise hydration processes of NO^+, with the "appropriate" isomeric structures of $NO^+(H_2O)_{n+1}$, $n + 1 = 1-3$ (see Figure 3), which lead to nitrous acid formation, are shown in Table 3. It should be noted that these "appropriate" structures are not the lowest-energy isomeric structures, except for $n + 1 = 1$. These structures arise from increasing the solvent chain bonded to $NO^+(H_2O)$ (structures C_1(b) and C_1(b)′ of Figure 3; these are structure C_1(b) in Figure 1 and structure C_1(b) in Figure 2 of ref 7). These structures are 1.16 and 3.03 kcal mol^{-1} above their respective lowest energy minimum (C_1(a) in Figure 1 and C_S(b) in Figure 2 of ref 7) at the MP2/aug-cc-pVTZ level. Nevertheless, it can been seen from the computed reaction enthalpies ($\Delta H°$) and free energies ($\Delta G°$) that each reaction step is thermodynamically favored at the MP2/aug-cc-pVTZ//MP2/6-311+G(2d,p) level (both $\Delta H°$ and $\Delta G°$ are negative) up to the $HONO{\cdot}H^+(H_2O)_3$ complex formation (reactions a−d in Table 3). However, the computed $\Delta H°$ and $\Delta G°$ values in Table 3 show that formation of nitrous acid and protonated water cluster as separate products, whether from the $HONO{\cdot}H^+(H_2O)_3$ complex (reaction e in Table 3) or the reactants (reaction f in Table 3), is thermodynamically unfavorable under standard state conditions (both $\Delta H°$ and $\Delta G°$ are positive). Nevertheless, with the addition of an extra water to the $HONO{\cdot}H^+(H_2O)_3$ complex (reaction g in Table 3), the production of nitrous acid and a protonated water cluster as separate products is now thermodynamically favored (both $\Delta H°$ and $\Delta G°$ are negative).

In the evaluation of the thermodynamic quantities for reaction g in Table 3, the lowest-energy isomer of $H^+(H_2O)_4$[12] was considered. The reactant and product ion−molecule intermediates for reaction g were also obtained at the MP2/6-311+G(2d,p) level, and their structures (and some important intermolecular geometrical parameters) are shown in Figures 1 and 2, respectively. Although we were unable to perform harmonic vibrational frequency calculations on these intermediates at the MP2/6-311++G(2d,p) level, as mentioned in the last section, the MP2/6-31++G** geometry optimization and frequency calculations carried out confirmed that they are true minima and hence reaction intermediates.

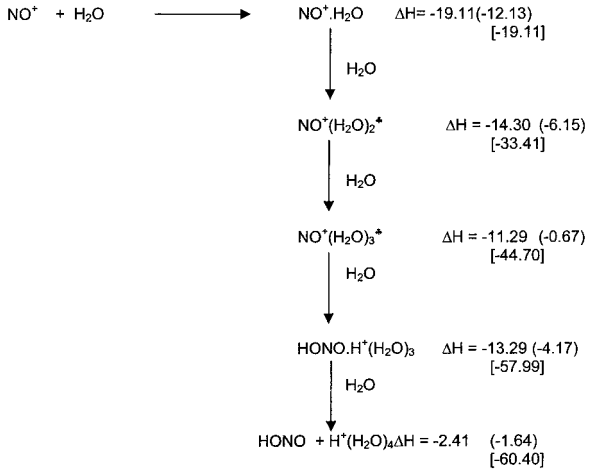

Figure 4. Overall reaction scheme and relative reaction energies for HONO and $H^+(H_2O)_4$. Values shown are $\Delta H°$ values in kcal/mol computed at the MP2/aug-cc-pVTZ//MP2/6-311++G(2d,p) level. Values shown in parentheses are associated $\Delta G°$ values in kcal/mol and those in brackets are the cumulative reaction enthalpy values in kcal/mol. The structures of $NO^+(H_2O)_n$ are those shown in Figure 3.

The computed electronic energy of the reactant intermediate with respect to the separate reactants is 13.19 kcal mol^{-1} with the former lying lower than the latter, while, relative to the product intermediate, the reactant intermediate is 0.58 kcal mol^{-1} higher, at the MP2/6-311+G(2d,p) level. A transition state between the reactant and product intermediates is expected. From Figures 1 and 2, to form the product intermediate from the reactant intermediate, the water molecule in the second solvation shell of $NO^+(H_2O)_4$ of the reactant intermediate is required to be inserted between the HONO and H_3O^+ moieties. Such a process would involve essentially breaking and forming of hydrogen bonds. In view of this consideration and the closeness of the computed electronic energies of the two intermediates, the activation energy required to form the transition state would not be expected to be unduly high. Because of the anticipated extremely demanding computational requirements, we did not attempt to locate a transition state structure, which would connect the reactant and product intermediates. Nevertheless, since the reactants are more than 13 kcal mol^{-1} higher in electronic energy than the reactant and product intermediates, the reacting system would probably have sufficient energy to overcome the activation barrier between the two intermediates. Therefore, it seems reasonable to suggest that the separate products of nitrous acid and protonated water cluster would very likely be produced at near collision rate from reaction g.

The steps involved in nitrous acid formation as well as their reaction enthalpies are summarized in Figure 4. They are reactions a−d and g in Table 3, and the structures of the complexes involved are shown in Figure 3. The first step is solvation of NO^+ by one water molecule. This is exothermic with a $\Delta H°$ value of −19.11 kcal.mol^{-1} (and a $\Delta G°$ value of −12.13 kcal.mol^{-1}). All of this excess energy will be retained in $NO^+(H_2O)$ unless collision with a third body (e.g. N_2) occurs to remove some of this internal energy. Also if, as is more likely, $NO^+(H_2O)$ formation occurs via collision of NO^+ first with N_2 to form $NO^+(N_2)$ followed by ligand exchange with H_2O, the excess energy content in $NO^+(H_2O)$ will be somewhat less than 19.11 kcal mol^{-1}. Most of the reaction energy is, however, expected to be retained in $NO^+(H_2O)$ as it corresponds to formation of a new bond. Similarly, solvation of $NO^+(H_2O)$ to give $NO^+(H_2O)_2$ and $NO^+(H_2O)_3$ via structures C_1(b) and C_1-

(b)′ of Figure 3 are also exothermic with $\Delta H°$ values of −14.30 and −11.29 kcal mol^{-1}. These structures correspond to increasing the solvent chain attached to NO^+ rather than filling the solvent shell around NO^+. Again, these $\Delta H°$ values are expected to be upper limits of the energy retained in the complex with solvation expected to occur in the upper atmosphere via $NO^+(H_2O)_n(N_2)$ formation followed by ligand exchange to give $NO^+(H_2O)_{n+1}$. Nevertheless, $NO^+(H_2O)_3$ has an enthalpy of −44.70 kcal mol^{-1} relative to the reactants ($NO^+ + 3H_2O$) and HONO·$H^+(H_2O)_3$ has an enthalpy of −57.99 kcal mol^{-1} relative to the reactants ($NO^+ + 4H_2O$). Even though these exothermicities are upper limits of the energy retained in the complex, there should be more than enough excess energy for reaction e ($\Delta H° = +15.2$ kcal mol^{-1}) or f ($\Delta H° = +2.03$ kcal mol^{-1}) to proceed.

Hence, overall the reaction scheme summarized in Figure 4 is sufficiently exoergic for the overall scheme to be thermodynamically feasible, even though the higher energy isomeric structures of $NO^+(H_2O)_2$ and $NO^+(H_2O)_3$ are involved (structures C_1(b) and C_1(b)′ in Figure 3). At equilibrium at 300 K, the percentages of these excited isomers are 14% and 0.6% relative to the most stable forms (C_1(a) in Figure 1 and C_s(b) in Figure 2 respectively of ref 7) and at 190 K, the approximate temperature of the upper atmosphere, these percentages reduce to 4.7% and 0.03%. However, these isomers are only 1.16 and 3.03 kcal mol^{-1} above the most stable $NO^+(H_2O)_2$ and $NO^+(H_2O)_3$ forms and there is sufficient excess reaction energy to convert the most stable form into the appropriate higher energy isomer prior to reaction. Hence, even though the populations of structures C_1(b) may be low in the upper atmosphere, there is enough available energy to convert the most stable $NO^+(H_2O)_2$ and $NO^+(H_2O)_3$ isomers into structures C_1(b) prior to the reactions shown in Figure 4 which produce HONO and $H^+(H_2O)_n$.

3.4. Further Investigation on Nitrous Acid Formation from the Reaction $H_2O + NO^+(H_2O)_n \rightarrow HONO + H^+(H_2O)_n$. To have a clearer understanding of nitrous acid formation in the stepwise hydration processes of NO^+, particularly with $NO^+(H_2O)_n$, where $n \leq 3$, the stability of HONO·$H^+(H_2O)_n$, where $n = 1$ and 2, was investigated. Geometry optimization calculations at the MP2/6-311++G(2d,p) level were carried out. The initial geometries employed in the optimization calculations were based on that of HONO·$H^+(H_2O)_3$ obtained previously in studying reaction d (see Table 3; structure C_1(b)″ in Figure 3). For both $n = 1$ and 2, geometry optimization of HONO·$H^+(H_2O)_n$ led to $NO^+(H_2O)_{n+1}$, where $n + 1 = 2$ and 3, respectively (C_1(b) structures in Figures 1 and 2 of part 1[7]). This suggests that HONO·$H^+(H_2O)_n$ is not stable for $n = 1$ and 2, as intracluster reactions convert nitrous acid-protonated water cationic complexes to hydrated NO^+ clusters with negligible activation barriers. The reaction profiles of the reaction $NO^+(H_2O)_n + H_2O \rightarrow HONO + H^+(H_2O)_n$, where $n = 2$ and 3, can be summarized as follows. Starting with an appropriate isomeric structure of $NO^+(H_2O)_n$, for $n = 2$, the separate reactants move to the energy valley of the reactant intermediate and then go to the separate products without a barrier nor a product intermediate. The overall reaction is endothermic by ca. 13 kcal mol^{-1}. However, for $n = 3$, with an appropriate isomeric structure of $NO^+(H_2O)_3$, the reactants go straight to the energy well of the product intermediate, HONO·$H^+(H_2O)_3$. The reaction surface possesses neither a reactant intermediate nor a barrier. The overall reaction is still endothermic, but only by 2 kcal mol^{-1} at the highest level of calculation (reaction in Table 3). Last, when the product intermediate of reaction f, HONO·$H^+(H_2O)_3$, reacts with one more water molecule, the overall reaction to the separate products of HONO + $H^+(H_2O)_4$ is now exothermic (reaction in Table 3) and the reaction surface consists of a reactant intermediate (Figure 1), a transition structure, and a product intermediate (Figure 2), similar to the reaction surfaces of many other ion−molecule reactions.

3.5. Relative Concentrations and K_P. Considering competition between $NO^+(H_2O)_{n+1}$ cluster formation (reactions 1, with $n + 1 = 1-4$ in Table 1) and nitrous acid formation (reactions a−d and g in Table 3), it would be desirable to deduce the relative concentrations of $NO^+(H_2O)_4$, HONO·$H^+(H_2O)_3$, and/or $H^+(H_2O)_4$. Following the approach reported in our previous study on protonated water clusters,[12] the concentration of various NO^+ hydrate clusters at equilibrium can be expressed as follows:

$$[NO^+(H_2O)_{n+1}] = [NO^+(H_2O)_n][H_2O]K_{n+1} = [NO^+][H_2O]^{n+1}K_1K_2 \ldots K_{n+1}$$

Here K_1, ..., and K_{n+1} are the equilibrium constants for reactions 1, with $n + 1 = 1-4$ in Table 1, respectively.

Similarly, for the formation of HONO·$H^+(H_2O)_3$ (Table 3),

$$[HONO\cdot H^+(H_2O)_3] = [NO^+\cdot(H_2O)_3][H_2O]K_4' = [NO^+][H_2O]^4K_1'K_2'K_3'K_4'$$

where K_1', K_2', K_3', and K_4' are the equilibrium constants for reactions a−d in Table 3, respectively. (Note that reaction 1, with $n + 1 = 1$ in Table 1, is identical to reaction a in Table 3, as both start with the lowest-energy isomer of $NO^+\cdot H_2O$; hence they have the same K_1.) From the above equations, the ratio between the concentration of $NO^+(H_2O)_4$ and HONO·$H^+(H_2O)_3$ can be expressed as

$$\frac{[NO^+(H_2O)_4]}{[HONO\cdot H^+(H_2O)_3]} = \frac{K_2K_3K_4}{K_2'K_3'K_4'}$$

At standard pressure and temperature, this ratio is 3360:1.

When the concentration of $H^+(H_2O)_4$ is considered, it can be expressed as following:

$$[H^+(H_2O)_4] = \frac{K_5'[H_2O][HONO\cdot H^+(H_2O)_3]}{[HONO]} = \frac{[NO^+][H_2O]^5K_1'K_2'K_3'K_4'K_5'}{[HONO]}$$

The ratio between the concentrations of $H^+(H_2O)_4$ and $NO^+\cdot(H_2O)_5$ is

$$\frac{K_2'K_3'K_4'K_5'}{K_2K_3K_4K_5[HONO]} = \frac{0.00619}{K_5[HONO]}$$

where K_5' is the equilibrium constant for reaction g in Table 3.

$H^+(H_2O)_3$ is produced by two routes, reactions e and f in Table 3. Reaction f is expected to dominate given its more favorable K_p value. However, if the equilibrium constants for these reactions are denoted as K_e and K_f, then the concentration of $H^+(H_2O)_3$ can be expressed as

$$H^+(H_2O)_3 = \frac{K_f[H_2O][NO^+(H_2O)_3]}{[HONO]} + \frac{K_e[HONO{\cdot}H^+(H_2O)_3]}{[HONO]}$$

$$= \frac{K_f K_1 K_2' K_3' [H_2O]^4 [NO^+]}{[HONO]} + \frac{K_e K_1 K_2' K'_4 [H_2O]^4 [NO^+]}{[HONO]}$$

The ratio $H^+(H_2O)_3/H^+(H_2O)_4$ can be expressed as

$$\frac{H^+(H_2O)_3}{H^+(H_2O)_4} = \frac{(K_3' K_f + K_e K_4')}{K_3' K_4' K_5' [H_2O]} = \frac{23.65 \times 10^{-3}}{K_3' K_4' K_5' [H_2O]}$$

With the K_p values listed in Table 3, obtained at the MP2/aug-cc-pVTZ//MP2/6-311++G(2d,p) level, then

$$\frac{H^+(H_2O)_3}{H^+(H_2O)_4} = \frac{2.77 \times 10^{-7}}{[H_2O]}$$

In the upper atmosphere the water partial pressure drops on increasing altitude from 70 to 90 km. The above equation indicates that this would lead to an increase in $[H^+(H_2O)_3]/[H^+(H_2O)_4]$ ratio with increasing height and this indeed observed experimentally.[13]

There are very few available laboratory measurements with which to compare the results of this present work. The most relevant experimental work is that of Stace et al.,[5,6] Okumura et al.,[4] and Kennedy et al.[14] In the work of Stace et al.,[5,6] neutral $NO(H_2O)_n$ clusters were ionized by electron impact and mass selected. Mass analyzed ion kinetic energy spectra were recorded for $NO^+(H_2O)_n$, following collisional activation, for each n in the range 2−9. Both metastable loss from $NO^+(H_2O)_n$ ions as well as collisionally activated loss was observed. It was found that for n =2 and 3 only water loss was observed from $NO^+(H_2O)_n$ as a result of both metastable loss and collisional activation. For $n = 4$, loss of HONO or H_2O was observed by metastable loss and collisional activation whereas for $n = 5$ HONO loss dominates relative to H_2O loss.

Related work has also been performed by Okumura and co-workers.[4] In these experiments, $NO^+(H_2O)_n$ ions are produced by a high-pressure, pulsed discharge and then cooled in a supersonic expansion. Infrared predissociation spectra were recorded on each ion cluster by exciting the ions in the wavenumber region 2700−3700 cm^{-1}. It is notable that the ion complexes generated in the work of Stace et al.[5,6] by electron impact of neutral clusters are likely to be more excited and hence have a higher internal energy content than those ions generated via supersonic expansion of an ion beam in the work of Okumura et al.[4] In the infrared predissociation experiments of Okumura et al.,[4] for each $NO^+(H_2O)_n$ ion, with $n = 1-4$, only infrared spectra of $NO^+(H_2O)_{n-1}$ ions were observed, consistent with H_2O loss, whereas for $NO^+(H_2O)_5$ a spectrum of $H_3O^+(H_2O)_3$ was recorded consistent with HONO loss.

In the work of Kennedy et al.,[14] NO^+ $v^+ = 0$ was produced via (2 + 1) REMPI via the C←X 2-photon transition and expanded with a high pressure of an inert gas doped with water vapor through a nozzle into a low-pressure region where the ion distribution was measured by a time-of-flight (TOF) mass spectrometer. TOF mass spectra are presented for the NO/inert gas mixture passed over a water reservoir held at −10 and −20 °C. Both mass spectra show signals from $H^+(H_2O)_n$, $NO^+(H_2O)_n$, and $(NO)^+_x(H_2O)_y$ ions, where $x = 2-4$ and $y = 0-3$. The spectrum recorded at −10 °C shows more extensive structure to higher mass-to-charge ratio.

A number of observations can be made from these spectra which are consistent with the results of this present work: (i) For $H^+(H_2O)_n$, the minimum value of n in the experimental spectra is 4, and for $NO^+(H_2O)_n$, the maximum observed value of n is $n = 5$. (ii) At −10 °C, $H^+(H_2O)_n$ signals are observed with relative intensities in the order $4 < 5 < 6 > 7$ whereas at −20 °C, where the water partial pressure will be lower, the observed order is $4 < 5$ with $n = 6$ and $n = 7$ not observed. It is particularly notable that $H^+(H_2O)_6 > H^+(H_2O)_5 > H^+(H_2O)_4$ at −10 °C but $H^+(H_2O)_5 \approx H^+(H_2O)_4$ with $H^+(H_2O)_6$ not observed at −20 °C. (iii) $(NO)_2^+(H_2O)_n$, $(NO)_3^+(H_2O)_n$, and $(NO)_4^+(H_2O)_n$ ions are observed indicating that other ion−molecule reactions need to be taken into account with the ion−molecule reactions, reactions 1 and 2, for a full treatment of this reacting system. (iv) For the $NO^+(H_2O)_n$ signals, at −10 °C the relative ion intensities are in the order $2 > 3 > 4 \gg 5$. This is also the order at −20 °C, but $n = 4$ and $n = 5$ signals are not observed. It is not possible to compare these experimental results with the results of the present work quantitatively as the ion concentrations at equilibrium have not been measured and the relevant thermodynamic constants have not been determined. Nevertheless qualitative comparisons can be made. Loss of HONO from $NO^+(H_2O)_5$ is reaction g in Table 3. This is favored both by the structure of the complex and the calculated negative standard free energy. Loss of HONO is exothermic whereas loss of water is endothermic. For $NO^+(H_2O)_4$, loss of HONO corresponds to reaction e whereas loss of H_2O is the reverse of reaction d. Both processes are endothermic and will compete with each other. For $NO^+(H_2O)_3$, loss of water is the reverse of reaction c ($\Delta G° = +0.67$ kcal/mol) whereas loss of HONO is much more endothermic. Hence, qualitatively the results of Stace et al.,[5,6] Okumura et al.,[4] and Kennedy et al.[14] can be understood based on the results of this work. There is however, a clear need for experimental measurements of the thermodynamic values of the stepwise hydration processes listed in Table 3 for comparison with the results of this present study.

4. Concluding Remarks

In this work, thermodynamic constants for the stepwise hydration processes of NO^+ (reaction 1) and the intracluster rearrangement reactions (reaction 2) have been computed by high level *ab initio* calculations. On the basis of the results obtained, the competition between reactions 1 and 2 for different values of n can be understood.

First, for the stepwise $NO^+(H_2O)_{n+1}$ cluster formation, on going to $n + 1 = 4$, there is in total 59.2 kcal mol^{-1} excess energy generated. For the series of cluster reactions leading to $HONO{\cdot}H^+(H_2O)_3$ shown in Figure 4, there is in total 58.0 kcal mol^{-1} excess energy. The excess energy may remain in the system and/or be lost via collisions with third bodies in the system. If the pressure is high, collisional deactivation would almost certainly occur. In this case, $NO^+(H_2O)_{n+1}$ cluster formation would dominate over nitrous acid formation, as each step of reaction 1 is thermodynamically more favorable than each step of reaction 2. On the other hand, at low pressure, where there are few collisions, the excess energy available in the system may make nitrous acid formation more favorable. This is because formally endothermic reactions, such as reactions f in Table 3, may now proceed with the excess energy available

in the system. Isomers above the lowest-energy form are likely to be formed with the excess energy available in the system. This also facilitates nitrous acid formation.

For $n = 1$ and $n = 2$, the results in Tables 1−3 show that the hydration reaction (reaction 1) dominates as reaction 1 is exothermic, with a negative $\Delta G°$, whereas reaction 2 is endothermic, with a positive $\Delta G°$. For $n = 3$ and $n = 4$, for reaction 1 $\Delta H°$ and $\Delta G°$ are less negative, and for reaction 2, $\Delta H°$ and $\Delta G°$ are less positive (see Tables 1 and 2). Hence if sufficient energy is retained in the $NO^+(H_2O)_n$ complex from the previous solvation reactions, the rearrangement reaction, reaction 2, is expected to contribute to the observed products. The structural changes that occur in this rearrangement process, reaction 2, have been established in this study and are shown schematically in Figure 3. Addition of the first water occurs onto the nitrogen end of the NO^+. The next two water molecules are added consecutively to increase the solvent chain to form $NO^+(H_2O)_3$. The fourth water molecule is also added to the solvent chain, but on formation of $NO^+(H_2O)_4$, a rearrangement occurs to give $HONO{\cdot}H^+(H_2O)_3$. If sufficient energy is available, this can dissociate to $HONO + H^+(H_2O)_3$. Alternatively, addition of another water to $HONO{\cdot}H^+(H_2O)_3$ gives $HONO{\cdot}H^+(H_2O)_4$ which on dissociation gives $HONO + H^+(H_2O)_4$ (see Figure 4).This last solvation and dissociation step is exothermic (see Table 3) and is expected to occur with collisional frequency.

Acknowledgment. Financial support from the EPSRC (U.K.) and the Leverhulme Trust is gratefully acknowledged.

References and Notes

(1) Wayne, R. P. *Chemistry of Atmospheres*; Oxford University Press: Oxford, U.K., 1991.

(2) Ferguson, E. E. *Geophys. Space Res.* **1971**, *9*, 997.

(3) Fehsenfeld, F. C.; Ferguson, E. E. *J. Geophys. Res.* **1969**, *74*, 5743.

(4) Choi, J.-H.; Kuwata, K. T.; Haas, B.-M.; Cao, Y.; Johnson, M. S.; Okumura, M. *J. Chem. Phys.* **1994**, *100*, 7153.

(5) Stace, A. J.; Winkel, J. F.; Martens, R. B. L.; Upham, J. E. *J. Phys. Chem.* **1994**, *98*, 2012.

(6) Angel, L.; Stace, A. J. *J. Chem. Phys.* **1998**, *109*, 1713.

(7) Hammam, E.; Lee, E. P. F.; Dyke, J. M. *J. Phys. Chem. A* **2000**, *104*, 4571.

(8) Boys, S. F.; Bernardi, F. *Mol. Phys.* **1970**, *19*, 553.

(9) Frisch, M. J.; Trucks, G. W.; Schlegel, H. B.; Gill, P. M. W.; Johnson, B. G.; Robb, M. A.; Cheeseman, J. R.; Keith, T.; Petersson, G. A.; Montgomery, J. A.; Raghavachari, K.; Al-Laham, M. A.; Zakrzewski, V. G.; Ortiz, J. V.; Foresman, J. B.; Cioslowski, J.; Stefanov, B. B.; Nanayakkara, A.; Challacombe, M.; Peng, C. Y.; Ayala, P. Y.; Chen, W.; Wong, M. W.; Andres, J. L.; Replogle, E. S.; Gomperts, R.; Martin, R. L.; Fox, D. J.; Binkley, J. S.; Defrees, D. J.; Baker, J.; Stewart, J. P.; Head-Gordon, M.; Gonzalez, C.; Pople, J. A. *Gaussian 94, revision D.4*; Gaussian, Inc.: Pittsburgh, PA, **1995**.

(10) French, M. A.; Hills, L. P.; Kebarle, P. *Can. J. Chem.* **1973**, *51*, 456.

(11) Burdett, N. A.; Hayhurst, J. *J. Chem. Soc., Faraday Trans. 1* **1982**, *78*, 2997.

(12) Lee, E. P. F.; Dyke, J. M. *Mol. Phys.* **1991**, *73*, 375.

(13) Brasseur, G.; Solomon, S. *Aeronomy of the Middle Atmosphere: Chemistry and Physics in the Stratosphere and Mesosphere*, 2nd ed.; Reidel: Dordrecht, The Netherlands, 1986.

(14) Kennedy, R. A.; Kung, C. Y.; Miller, T. A. In *Ion and Cluster Ion Spectroscopy and Structure*; Maier, J. P., Ed.; Elsevier: Amsterdam, 1989; p 213.